Approach for sizing by optimization of an electrical drive considering a multiphysics and multidynamics behaviour

Robin Thomas, Laurent Gerbaud, Hervé Chazal, Lauric Garbuio

Approach for sizing by optimization of an electrical drive considering a multiphysics and multidynamics behaviour

Robin Thomas , Laurent Gerbaud , Herve Chaza , Lauric Garbuio
Univ. Grenoble Alpes, CNRS, Grenoble INP, G2Elab, 38000 Grenoble, France

ABSTRACT

Purpose – The paper describes a modelling and solving methodology of a {static converter – electric motor – control} system for its sizing by optimisation, considering the dynamic thermal heating of the machine.

Design/methodology/approach – The electrical drive sizing model is composed of two simulators (electrical and thermal) that are co-simulated with a master-slave relationship for the time step management. The computation is stopped according to simulation criteria.

Finding – The paper details a methodology to represent and size an electrical drive using a multiphysics and multidynamics approach. The thermal simulator is the master and calls the electrical system simulator at a fixed exchange time step. The two simulators use a dedicated dynamic time solver with adaptive time step and event management. The simulation automatically stops on pre-established criteria, avoiding useless simulations.

Research limitations/implications – The paper aims to present a generic methodology for the sizing by optimisation of electrical drives with a multiphysics approach, so the precision and computation time highly depend on the modelling method of each components. A genetic multiobjective optimization algorithm is used.

Originality/value – The approach enables to compute a maximum operating duration before reaching thermal limits and to use it as an optimization constraint. These system considerations allow to over constrain the electrical machine, enabling to size a smaller machine while guaranteeing the same output performances.

Practical implications – The methodology can be applied to size electrical drives operating in a thermally limited zone. The power electronics converter and electrical machine can be easily adapted by modifying their sub-model, without impacting the global model and simulation principle.

Keywords: electrical drive, thermal heating, multiphysics modelling, time co-simulation, sizing by optimization

Paper type: research paper

INTRODUCTION

Electrical drives are sophisticated systems made of components of different nature: power electronics, electrical machine and control. In addition to the electromagnetic aspects, it is essential to consider the thermal behaviour of the machine to ensure accurate sizing of these systems with reliable performance calculations. This is particularly important since thermal heating remains one of the main constraints limiting the operation of electrical drives. Thus, the sizing by optimization of these systems implies to consider a multiphysics but also multidynamics approach (milliseconds for electrical aspects versus tenth of seconds for thermal aspects), raising complex modelling and solving issues.

The choice of the optimization algorithm impacts directly the choice of the modelling and solving methods, since it imposes computation constraints. The choice is among:

- gradient-based algorithms (e.g. SQP (Boggs and Tolle., 1995)) that enable to consider numerous sizing constraints and parameters, but require the implementation of the gradient computation with the issue of local minima;
- genetic algorithms that are easier to implement for global optimization but more time consuming, limiting the amount of sizing constraints that can be considered.

In the context of electrical drive applications, the following questions arise.

- How to choose which sub-components to model?
- How to represent them accurately while complying with optimization constraints?
- How to couple them?
- Furthermore, the analysis of dynamic physical behaviours requires their dynamic time simulation to be implemented, which means choosing which solver to use?
- How can the time step be managed when very different dynamics are being represented?

In order to preserve the possibility of using deterministic algorithms, the question also arises of how to compute the derivatives, but the paper does not deal with this aspect, even if a great part of the modelling can be derivated without using finite differences. This aspect will be discussed at the end of the paper.

Thus, the paper presents a methodology for the modelling and solving of a {static converter – squirrel cage induction motor – control} system for its sizing by optimisation, considering the dynamic heating of the machine in transient or steady state. After introducing the considered sizing by optimization problem, the paper presents the global sizing model principle. The modelling is then divided into two parts, with a description of the electrical circuit simulator and then the thermal simulator, before detailing the coupling principle and the co-simulation process. Finally, sizing by optimization results are shown to illustrate the presented methodology and compare the computation times.

I. STUDIED PROBLEM ANALYSIS

I.1 DESCRIPTION OF THE STUDIED PROBLEM

The presented problem consists in sizing the components of an electrical drive, composed of a power supply, a power electronics converter and an induction motor with its control, and considering its dynamic thermal heating. Figure 1 presents the bloc diagram of the considered system.

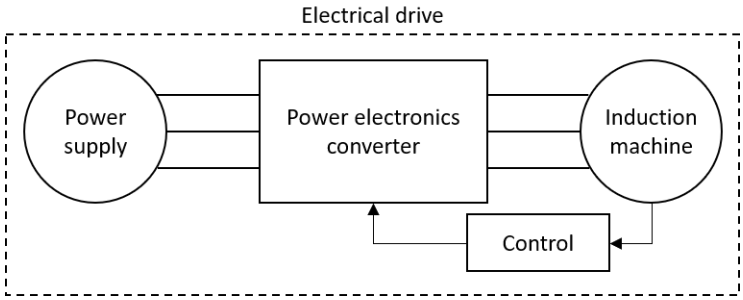

Figure 1: Block diagram of a classical electrical drive

The system is sized at electrical steady state operating points exceeding the continuous operating limits of the machine, i.e. in the classical thermally limited area of operation (Assaad *et al.*, 2017) as it is shown in figure 2.

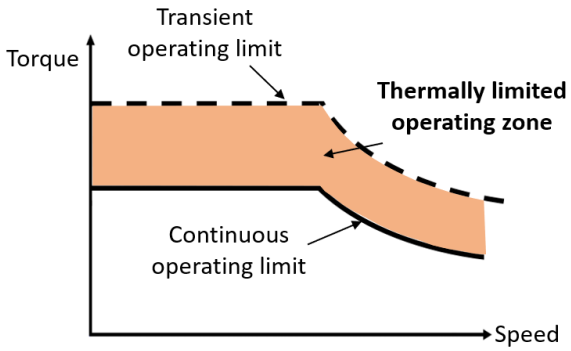

Figure 2: Operating limitations of an electric motor

The aim of this study is to size the electrical drive to ensure that it can operate at specific points exceeding the classical limits, for a minimum duration before reaching maximum temperatures inside the induction motor. Thus, temperature thresholds are imposed and short operating times with high thermal constraints are studied to characterize thermal transients (i.e. response times).

This sizing by optimization study takes place at the predesign phase, when engineers have to make choices, evaluate solutions and define specifications (Ulrich and Eppinger, 2011). Thus, the focus is made on medium-fidelity modelling with low computational cost, so that a large number of technical choices can be rapidly evaluated.

I.2 MODELLING AND SOLVING CONSTRAINTS

In order to be able to simulate the considered electrical drive, with the aim of sizing it, its multiphysics model needs to be composed of three main sub-models (cf. figure 3):

- a static electromagnetic model of the induction motor;
- a dynamic model of the static converter – induction motor drive operating at steady state;
- a dynamic thermal model of the induction motor in transient state. The thermal behaviour of the power electronics converter is not considered, i.e. the converter is supposed to be sized for a thermal steady-state.

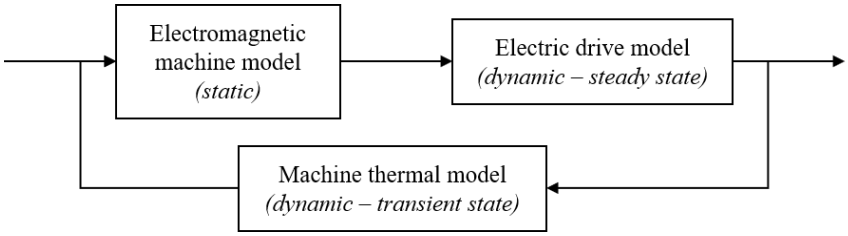

Figure 3: Block diagram of the electrical drive model

Then, the coupling between these sub-models must also be implemented.

The choice of the optimisation algorithm (stochastic, deterministic) impacts directly the modelling method and the simulation tools used (computation time, derivatives…). To limit the computation time in the predesign step, the implementation of "light" models, such as analytical models, is chosen. Moreover, to preserve the possibility of using gradient-based methods (like SQP), the computation of each model gradients needs to be implemented, using exact derivation when it is possible or finite differences.

Since the aim is to study the thermal heating of the machine when it is operating at specific points, the system has to be simulated dynamically. The dynamic simulation of a multiphysics problem can be carried out:

- using one global solver but with a total simulation time imposed by the slowest dynamics (i.e. the thermal dynamics), possibly leading to an unacceptable computation time cost for optimisation problems due to the large gap between the physical dynamics (milliseconds compared to seconds). A common solution is to transform the dynamic thermal constraint into a static constraint (Touhami *et al.*, 2020). However, this is not relevant for our case: the study of thermal dynamics and the crossing of temperature thresholds (critical limits);
- using a co-simulation with several solvers dedicated to the different physical dynamics.

This last solution is chosen.

The use of commercial solvers is possible, but they often have the disadvantage of being locked. This characteristic leads to limited driving capacity. Yet, in order to limit the computation time (regardless of the chosen optimisation method), it is essential to be able to detect when temperature thresholds are crossed (or a steady state is reached) and to stop the simulation at that time, avoiding unnecessary computations. Thus, an open time solver is developed for that purpose (Gerbaud *et al.*, 2021) and it enables to control the co-simulation process and implement temperature thresholds and steady-state detection. This solver is used in two simulators, to deal

on one part with the electrical system performances and on another part with the thermal heating of the machine. A specific methodology is set up to co-simulate these simulators.

II. PRINCIPLE OF THE GLOBAL SIZING MODEL

The principle of the global electrical drive sizing model and the coupling between the two simulators are presented in figure 4.

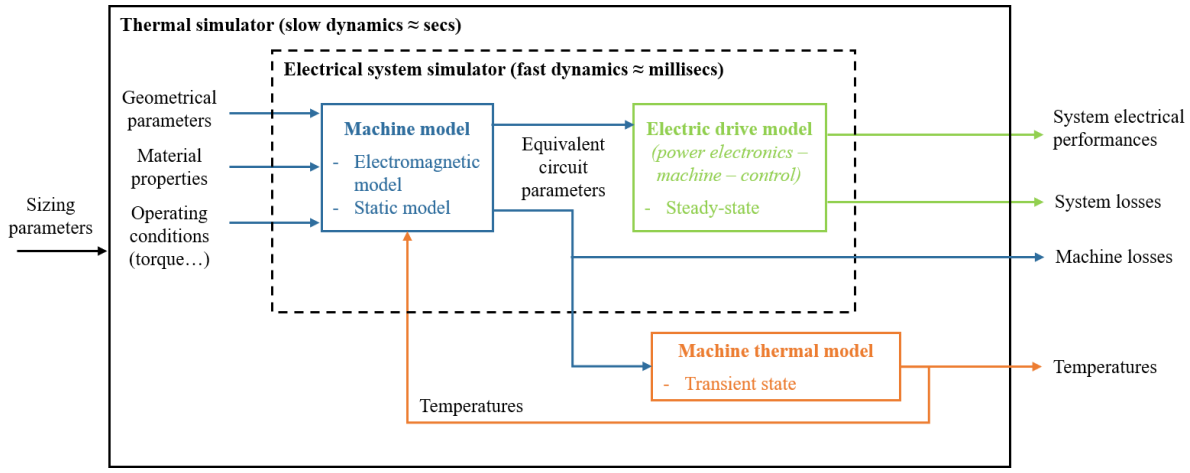

Figure 4: Architecture of the electrical drive sizing model

The first simulator is set up for the elements with fast dynamics (milliseconds), i.e. the machine and electrical drive models. The induction motor model aims to provide the parameters of the machine equivalent circuit and the needed current to the electrical drive model, considering the machine geometry, the chosen steady state operating conditions (torque, speed) and the temperatures. It is a static model. After simulation, the electrical drive model provides the overall performances (output power, voltage/current rms and max values) and the losses as outputs.

The second simulator is set up for the slow dynamics components (several tenth of seconds), i.e. the thermal model. It takes the geometrical parameters of the machine and its losses as inputs. After simulation, it provides the temperatures through the machine and the maximal operating time as outputs.

The content of each sub-model and the derivative computation method are depicted in the following sections.

III. ELECTRICAL DRIVE MODELLING

III.1 ELECTRICAL MACHINE SIZING MODEL

III.1.1 Model presentation and hypotheses

Considering the previously described constraints, the chosen induction motor model is a static behavioural analytical model, enabling to compute the equivalent diagram parameters using the machine geometry and the material properties (Zhu *et al.*, 2010) (cf. figure 5). It uses theoretical and empirical equations to describe the impact of several electromagnetic phenomena occurring in the machine (saturation, skin effect…) on the output performances (Liwschitz-Garik and Whipple, 1946), (Kostenko and Piotrovsky, 1969), (Alger, 1970), (Cochran, 1989). Among all the induction machine equivalent circuits available, the equivalent single-phase Y-connected T diagram, shown in figure 5, is chosen.

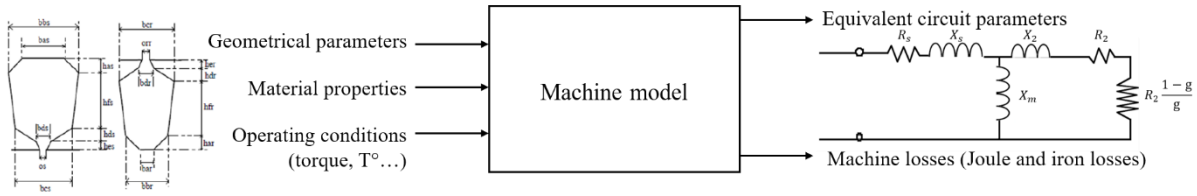

Figure 5: Electrical machine model principle

The main modelling hypotheses are:

- only the fundamental flux and steady state operating conditions are considered;
- no-load saturation effect in the magnetic circuit is considered using a corrective coefficient k_{sat};
- skin effect in rotor bars is considered;

III.1.2 Model structure

The implemented model is composed of five main steps and its structure is presented in figure 6.

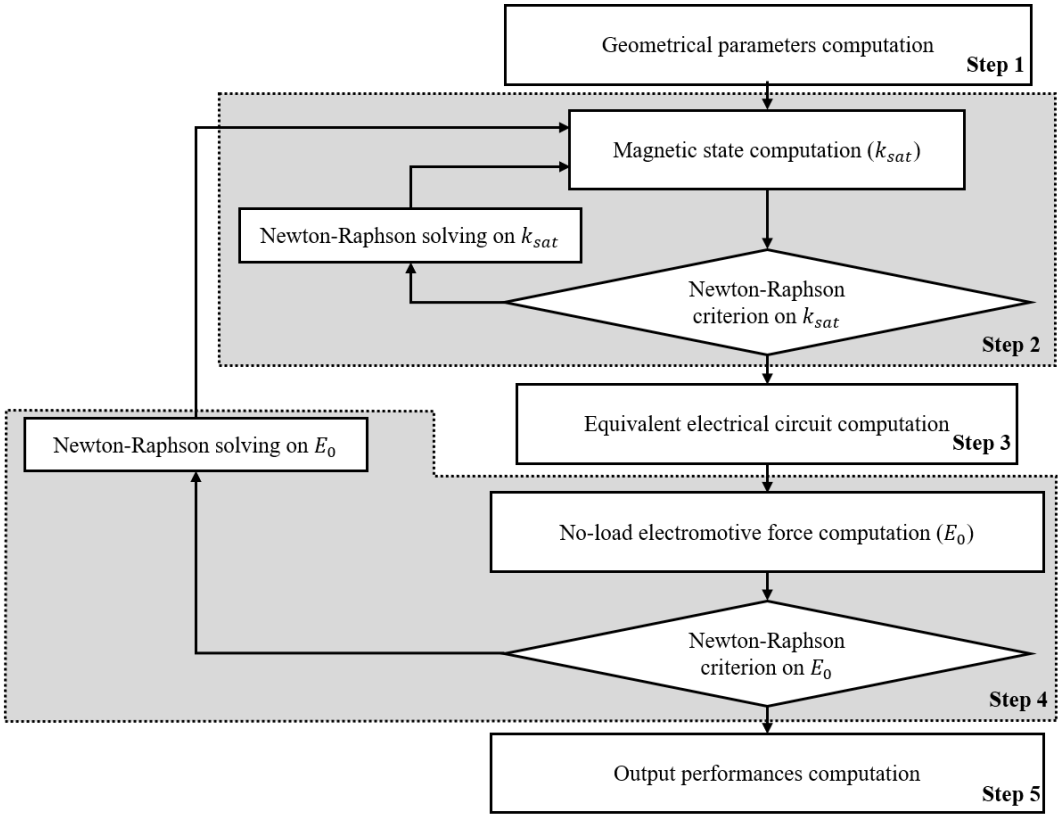

Figure 6: Induction machine static model structure

Step 1 – The geometrical parameters (volumes, sections…) are computed using the input values: machine inner and outer diameters, airgap width, stator and rotor slot dimensions and machine length.

Step 2 – The no-load magnetic state is estimated in order to compute the k_{sat} coefficient. This corrective coefficient represents the ratio between the magnetic potential difference needed to make the magnetic flux circulate through the airgap and the machine magnetic circuit, and the magnetic potential difference needed to make it flow only through the airgap (Liwschitz-Garik and Whipple, 1946):

$$k_{sat} = \frac{H_a(k_{sat}) \cdot l_a + H_s(k_{sat}) \cdot l_s + H_r(k_{sat}) \cdot l_r}{H_a(k_{sat}) \cdot l_a} \quad (1)$$

Where:

- H_k the magnetic field (k=a: airgap, k=s: stator, k=r: rotor);
- l_k the equivalent length (k=a: airgap, k=s: stator, k=r: rotor).

Thus, this coefficient equals 1 when the machine is unsaturated and increases with the saturation level. It can be observed that computing this coefficient requires solving an implicit loop.

To compute the magnetic field through each part of the machine, the equivalent magnetic flux under a pole is computed using the stator winding parameters and the electromotive force applied on the windings:

$$\phi_p = \frac{E_0}{4 \cdot k_f(k_{sat}) \cdot k_b \cdot f \cdot N_s}$$	(2)

Where:

- E_0 the no-load electromotive force. This parameter depends on the stator voltage drop and cannot be known at this step. Thus, an initial value is imposed and this second implicit loop will be solved at the step 4 of the machine model;
- $k_f(k_{sat})$ a corrective coefficient depending on k_{sat} (Liwschitz-Garik and Whipple, 1946);
- k_b the winding coefficient;
- f the frequency;
- N_s the number of turns.

This flux value is used to compute the flux density at different locations in the machine stator and rotor and in the airgap:

$$B_k = \frac{\phi_p}{S_k \cdot \alpha_i(k_{sat})}$$	(3)

Where:

- B_k the flux density across a section k of the machine magnetic circuit;
- S_k the surface of the section k;
- $\alpha_i(k_{sat})$ a corrective coefficient depending on k_{sat} (Liwschitz-Garik and Whipple, 1946);

Then, the magnetic field is computed using the B(H) magnetic characteristic of the considered electrical steel.

The implicit solving of the k_{sat} equation is made using a Newton-Raphson method, whose evolution equation and stopping criterion are:

$$k_{sat_{n+1}} = k_{sat_n} - \frac{\epsilon_{ksat_n}}{d\epsilon_{ksat_n}}$$	(4)
$$\sqrt{\left(\frac{\epsilon_{ksat_n}}{d\epsilon_{ksat_n}}\right)^2} < e$$	(5)

Where:

- $\epsilon_{ksat_n} = \sqrt{\left(k_{sat_n} - k_{sat_{n-1}}\right)^2}$;
- $d\epsilon_{ksat_n}$ the variation of $\epsilon_{k_{sat}}$ between the iterations n et n-1;
- e the chosen precision for the Newton-Raphson algorithm.

Step 3 – The elements of the equivalent circuit of the induction machine are computed. The resistances are calculated using the conductor geometry and the winding / bar temperatures. These temperatures are obtained from the machine thermal model and updated during the overall electrical drive model solving.

The leakage inductances are computed by identifying the leakage paths through the slots (ϕ_{1-4} on figure 7), but also considering tooth-tip, belt and zig-zag leakages (ϕ_5 on figure 7) (Belot, 1982), (Cordovil and Chabu, 2016).

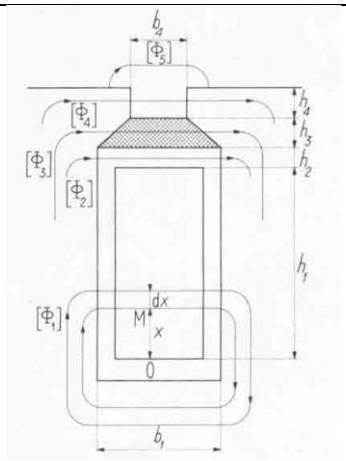

Figure 7: Location of the different leakage flux in a semi-closed slot (Belot, 1982).

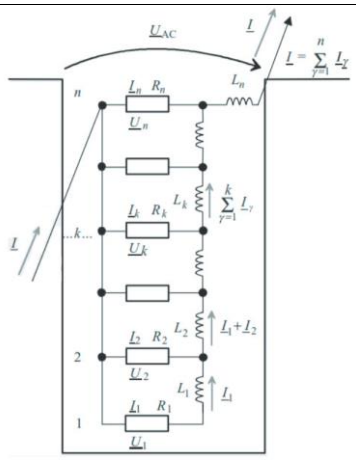

Figure 8: Equivalent circuit of a rotor slot divided into elementary sub-conductors (Maddi and Aouzellag, 2017).

In order to consider the skin effect in the rotor bars, each bar is divided in N layers and the equivalent circuit of each of these layers is written (cf. figure 8). The rotor resistance and inductance are computed using the total Joule losses and the total magnetic energy stored in all these layers (Boglietti *et al.*., 2011), (Maddi and Aouzellag, 2017).

The magnetizing inductance is computed using the electromotive force and the winding parameters, through the computation of the magnetizing current (Alger, 1970). The iron loss resistance is also computed, using a Bertotti model for the iron loss computation.

Step 4 – The resulting value of the no-load electromotive force is computed using the equivalent impedance of the machine and the applied voltage. The initially chosen value is corrected through the solving of the implicit loop. The Newton-Raphson algorithm used is the same as the one used at the step 2.

Step 5 – Finally, the machine performances are determined using the classical power diagram of an induction motor (cf. figure 9).

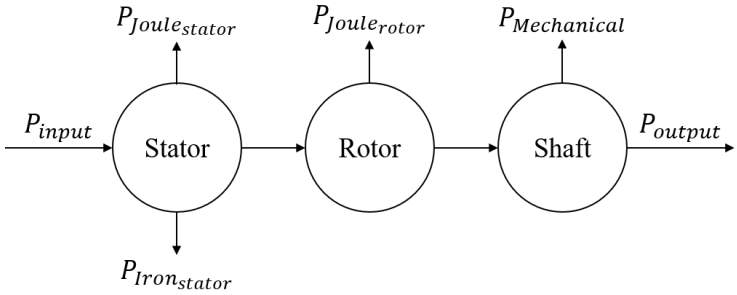

Figure 9: Induction motor power tree.

The outputs of the machine model are the values of the equivalent electrical circuit components and the performances, i.e. output power, stator and rotor Joule losses and iron losses.

III.2 ELECTRICAL DRIVE CIRCUIT MODEL

The model of the electrical drive uses its electrical circuit, comprising the power electronics converter circuit and the induction machine equivalent circuit. The switches of the static converter are considered ideal. This electrical circuit is described with its linear state equations, that can be written for any application as:

$$\begin{cases} \frac{dX}{dt}(t) = A(P) \cdot X(t) + B(P) \cdot u(P,t) \\ Y(t) = C(P) \cdot X(P,t) + D(P) \cdot u(P,t) \end{cases} \quad (6)$$

Where:

- t is the time;
- X is the state vector, Y is the output vector, $P = \{P_i, i = 1 \dots n_P\}$ is the sizing parameter vector and u represents the state inputs;
- A, B, C and D depend directly on P.

However, to consider the changes in the circuit topology due to the power electronics switchings (controlled and natural), the state equations needs to be written in pieces. The resulting piecewise system contains one state equations per existing state of the static converters and an event management needs to be implemented to manage these changes.

III.3 ELECTRICAL DRIVE SIMULATOR

III.3.1 Implementation of a dedicated solver

The numerical solving of the electrical drive state equations is achieved by implementing a dedicated dynamic solver (Gerbaud *et al.*, 2022). This solver uses Runge-Kutta 44 method (order 4 and more), with an adaptive time step. As a reminder of the principle behind this well-known method (Press *et al.*, 1992), it uses at least a 4th-order formula to evaluate the time derivatives four times (minor steps) per time step (major steps), as shown in figure 10.

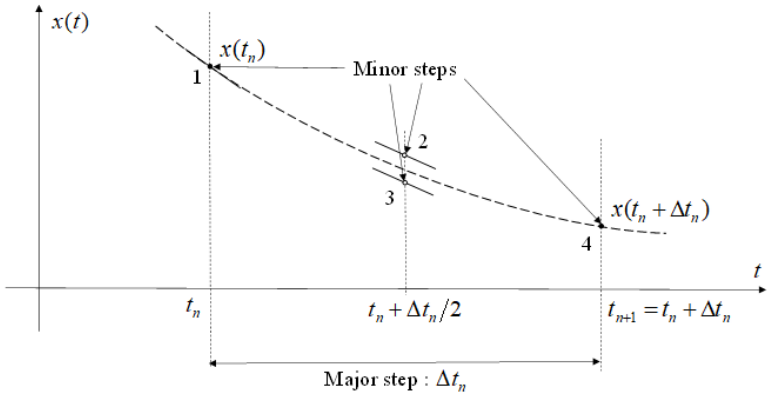

Figure 10: Steps of the Runge-Kutta 44 method (Gerbaud *et al.*, 2022).

However, several other adaptive Rung-Kutta methods can possibly be used by the implemented solver (e.g. RK45, 56) (Dormand and Prince, 1980).

III.3.2 Event management

An event management strategy is implemented to detect the switchings of the power electronics converter (controlled and natural) in order to adapt the time step and change the state equations. The implemented strategy relies on the prediction of events by combining zero-crossing approach with event managements, as described in paper (Gerbaud *et al.*, 2022).

III.3.3 Performance criteria and derivatives computation

The electrical drive performance criteria are the rms and maximum values of currents and voltages through the system. In addition, a power electronics loss model is implemented (conduction and commutation). These performance criteria are computed once the steady-state is reached, on one operating period. The simulation stops automatically, thanks to the event management strategy, once these criteria are computed, in order to avoid useless simulations.

IV. THERMAL BEHAVIOUR MODELLING

IV.1 ELECTRICAL MACHINE THERMAL MODEL

IV.1.1 Model presentation and hypotheses

The implemented thermal model is a lumped-parameter model enabling to reach high precision with limited computation time (Boglietti *et al.*, 2009). This model takes the geometrical dimensions of the machine and its losses as inputs to compute the value of the equivalent circuit components and heat sources. Then, this circuit is solved to compute the temperatures in each part of the machine, especially in the conductors (stator windings and rotor bars).

Each part of the machine (i.e. carter, stator and rotor yokes, windings…) is represented separately with an equivalent thermal circuit, including the cooling system (i.e. the stator cooling jacket and the rotor hollow shaft). The dynamic evolution of the temperature in each of these parts is represented using thermal capacitors. All the thermal sub-circuits are then connected together to form the overall model of the machine.

The main modelling hypotheses are:

- uniformity of properties, exchange conditions and heat sources;
- the temperatures are considered symmetrical with respect to the axial plane. The model deals with only one half of the machine;
- thermal transfers by radial, axial (and orthoradial) conduction and by convection are considered. Contact resistances and radiation transfers are neglected.

IV.1.2 Model structure

IV.1.2.1 Global equivalent thermal circuit

The implemented thermal circuit is presented in figure 11.

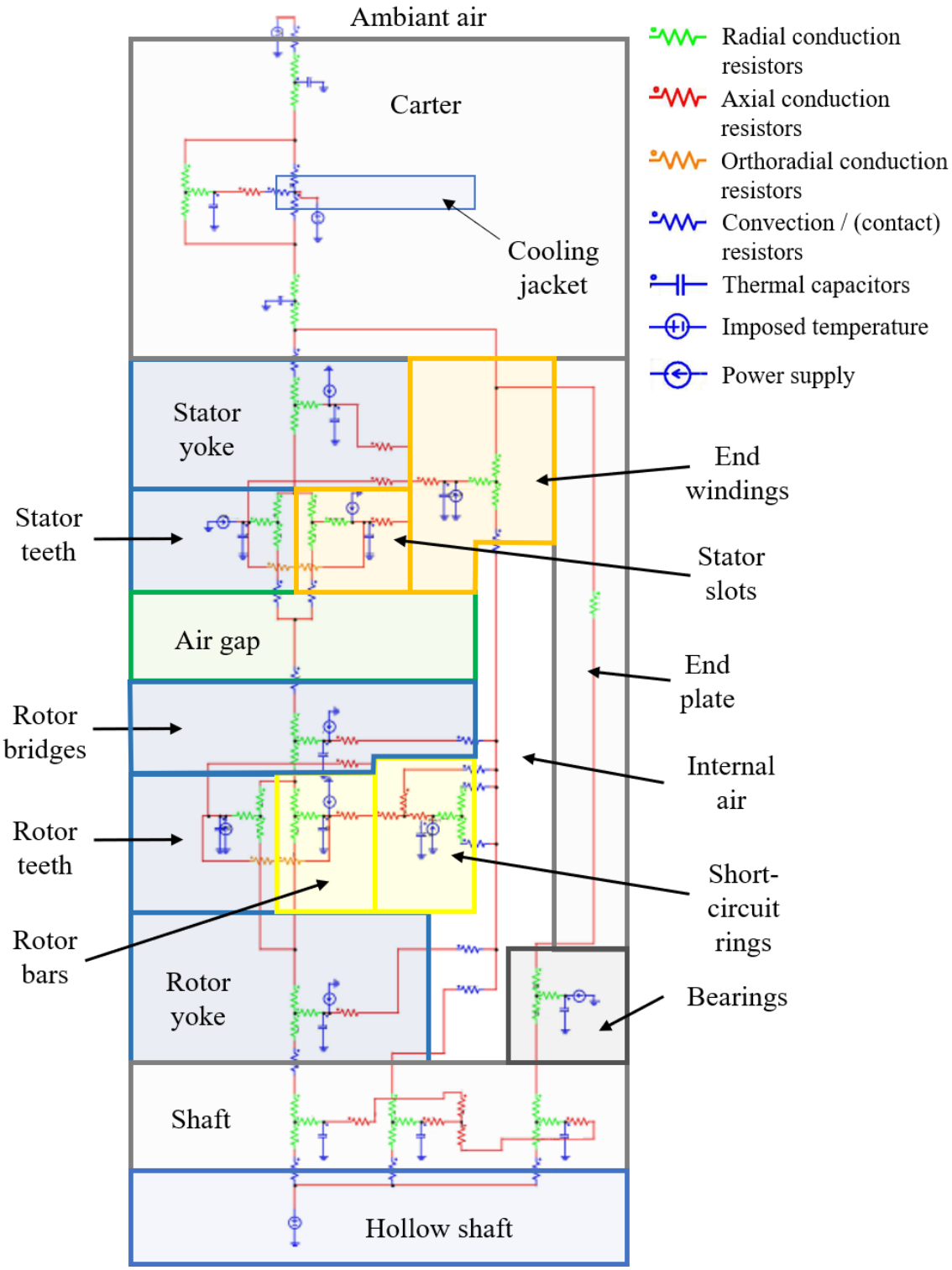

Figure 11: Equivalent thermal circuit of the induction motor.

IV.1.2.2 Thermal conduction resistances computation

The computation of the thermal conduction resistances is made by assimilating every part of the machine as a full (or a part) of a hollow cylinder, as it is depicted in figure 12.

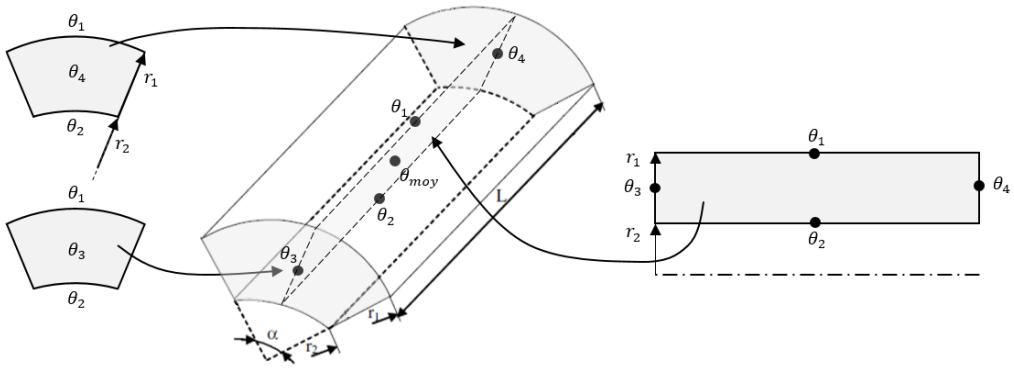

Figure 12: 3D representation of a part of a hollow cylinder.

This equivalent cylinder is then represented by the equivalent circuit shown in figure 13 (Mellor *et al.*, 1991), (Mezani *et al.*, 2005).

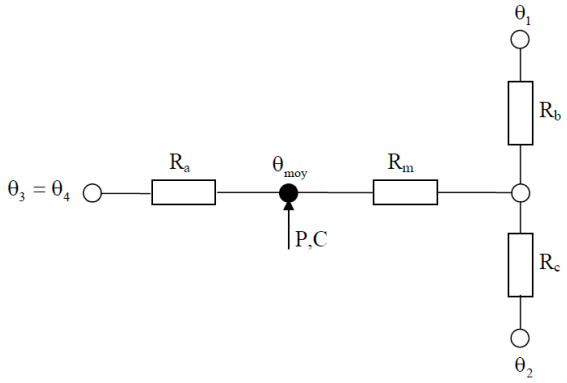

Figure 13: Simplified equivalent thermal circuit of a hollow cylinder.

$$R_a = \frac{L}{3 \cdot \alpha \cdot k_a \cdot (r_1^2 - r_2^2)}$$	(7)
$$R_b = \frac{1}{\alpha \cdot k_r \cdot L} \cdot \left(1 - \frac{2 \cdot r_2^2 \cdot \ln\left(\frac{r_1}{r_2}\right)}{r_1^2 - r_2^2} \right)$$	(8)
$$R_c = \frac{1}{\alpha \cdot k_r \cdot L} \cdot \left(\frac{2 \cdot r_1^2 \cdot \ln\left(\frac{r_1}{r_2}\right)}{r_1^2 - r_2^2} - 1 \right)$$	(9)
$$R_m = -\frac{1}{2 \cdot \alpha \cdot k_r \cdot (r_1^2 - r_2^2) \cdot L} \cdot \left(r_1^2 + r_2^2 - \frac{4 \cdot r_1^2 \cdot r_2^2 \cdot \ln\left(\frac{r_1}{r_2}\right)}{r_1^2 - r_2^2} \right)$$	(10)

Where:

- k_a and k_r are the material thermal conductivities in the axial and radial directions;
- L is the total length of the machine;
- r_1 and r_2 are the outer and inner radii of the cylinder.

The thermal conductivities depend on the material properties. For non-homogenous cases, such as the stator windings that are made of copper, varnish or resin, an equivalent conductivity is computed using a homogenisation formula (Zeaiter *et al.*, 2018), (Liu *et al.*, 2019).

IV.1.2.3 Thermal convection resistances computation

The convection thermal resistances, at the interface between a solid and a fluid, are computed from the Newton's formula (Holman, 2010):

$$R_{th_{conv}} = \frac{1}{h \cdot S} \quad (12)$$

Where:

- h is the exchange coefficient;
- S is the exchange surface.

The value of the exchange coefficient h is obtained using the Nüsselt's dimensionless number (Holman, 2010):

$$Nu = \frac{h \cdot d}{k} \quad (13)$$

Where:

- d is the characteristic dimension of the flow;
- k is the thermal conductivity of the fluid.

The value of the Nüsselt's number highly depends on the type of flow (laminar, turbulent or vortex) and is obtained from experimental correlations (Mills, 1999), (Staton *et al.*, 2005), (Fénot *et al.*, 2011).

IV.1.2.4 Thermal capacitors computation

The thermal capacitors, representing the heating dynamics of the machine, are computed by:

$$C_{th} = C_p \cdot \rho \cdot \frac{V_{region}}{2} \quad (14)$$

Where:

- C_p and ρ are the mass heat capacity and the density of the material;
- V_{region} is the volume of the considered part of the machine.

The resulting thermal circuit is composed of 106 elements (resistors, capacitors, heat and temperature sources).

IV.2 THERMAL SIMULATOR

After computing the value of the equivalent thermal circuit elements, the circuit is put into equations by an automatic model generation tool (Bordry and Foch., 1985), (Baraston *et al.*, 2016). Due to the size of the circuit, putting it into equations is very complex and this tool is used to write the numerical state matrices from the thermal circuit netlist, and to modify them if component values have changed. Figure 14 depicts this principle.

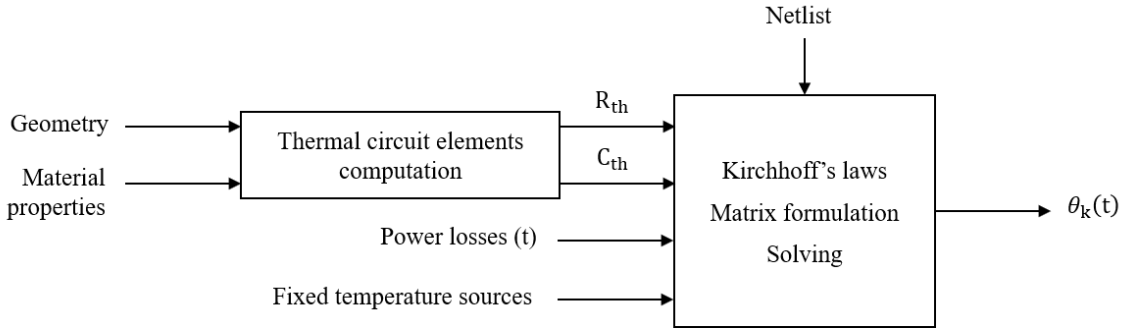

Figure 14: Thermal model generation principle.

The resulting state matrices are solved using the same kind of dynamic solver than the one used for the electrical system simulation, i.e. with adaptative time step and event management.

V. CO-SIMULATION PROCESS AND IMPLEMENTATION

V.1 COUPLING AND CO-SIMULATION PRINCIPLE

The co-simulation principle is depicted in figure 15. It can be observed that the dynamic electrical system simulator is encapsulated in the dynamic thermal simulator, which acts as the master for the time step management in order to synchronize the two solvers.

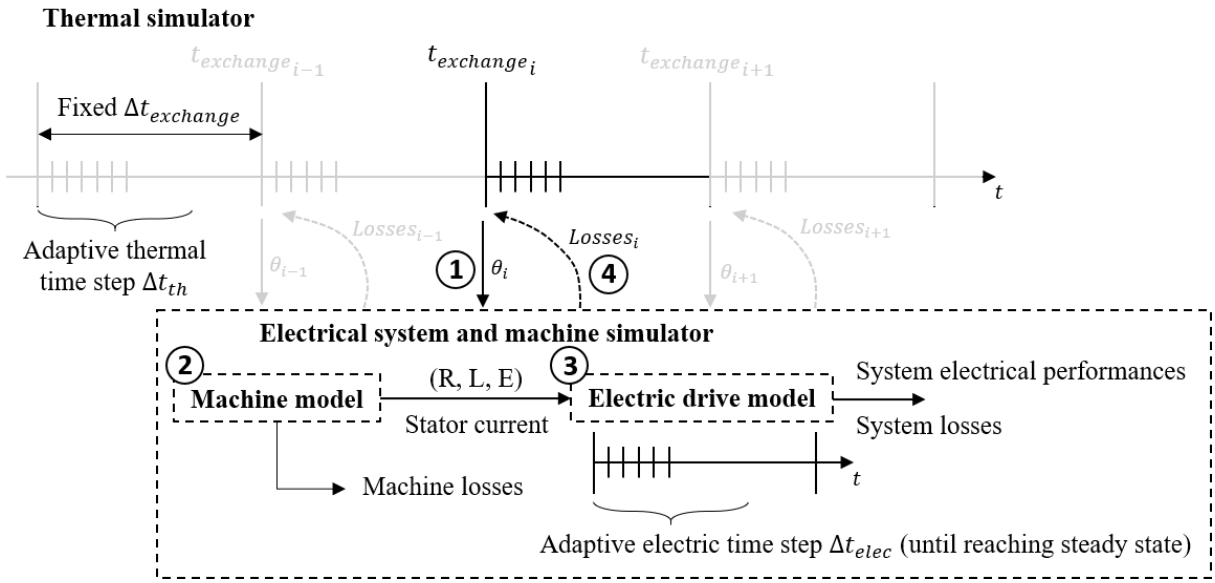

Figure 15: Co-simulation principle.

The co-simulation process is based on the following steps (with corresponding bubbles in figure 15):

1 – the thermal simulator calls the electrical system simulator at a fixed exchange time step $\Delta t_{exchange}$ to re-evaluate the losses in the machine, by giving it the new temperature values in the stator and rotor conductors;

2 – the machine sizing model is computed to update the values of the machine equivalent electrical circuit;

3 – the electrical system is simulated on a few periods with its adaptive time step Δt_{elec} until steady-state is reached and electrical performances are computed;

4 – the thermal model updates its heat sources and is then simulated with its own adaptive time step Δt_{th}, until the next exchange time is reached.

The simulation stops on three cumulable criteria:

- the final (maximum) duration is reached;
- one of the temperature thresholds is crossed;
- a steady state is detected.

The resulting simulation time t indicates the possible operating duration for the system, without reaching a temperature limit. This value can be used as a sizing by optimization constraint or parameter.

V.2 Implementation

The overall electrical drive sizing model has been implemented using CADES framework (Delinchant *et al.*, 2007). This framework enables to couple different models by exploiting the concept of software components. The machine static model is implemented in C language, while the power electronics model, the electrical drive simulator and the thermal simulator, are implemented in Java language. The coupling of these sub-models is implemented in SML language.

VI. Sizing by optimization example

VI.1 Study case

As the paper focuses on the modelling methodology, the optimization results presented will not be commented on, but will be used to illustrate the sizing methodology by using a multiobjective optimization algorithm: the well-known stochastic algorithm NSGA-II.

The study case is an induction machine fed by an inverter associated with a flying capacitor converter (Isobe *et al.*, 2007), (Cheng *et al.*, 2012). This converter is described using the modelling methodology presented in the paper, considering ideal switches and semi-conductor loss (conduction and switching). The presented event management strategy is used to switch between the state equations representing the different static converter states.

VI.2 Results

This study aims to analyse a trade-off between the static converter capacitor sizing and the machine sizing, when it runs at a chosen operating point while considering its dynamic heating.

There are 12 sizing parameters: 2 for the capacitors sizing and 10 for the machine sizing, with the use of homothetic coefficient. The constraints are that the machine is operating at a steady-state operating point beyond its continuous limits and the operating time has to be superior to 60 seconds before reaching temperature thresholds inside the stator windings and the rotor bars. Figure 16 shows the obtained results.

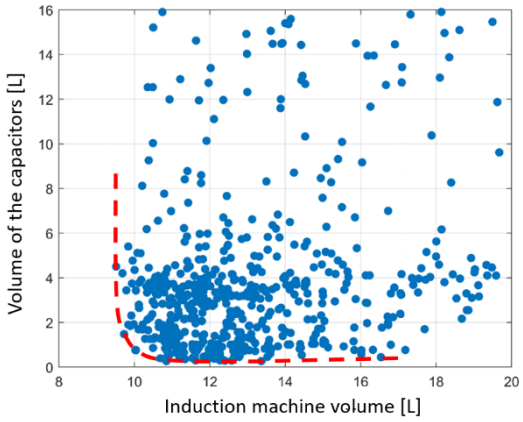

Figure 16: Optimization results for the capacitor sizing without considering thermal constraints.

To obtain these results, it took a few tens of minutes for one optimization and approximately one week to draw the Pareto front, with a PC Windows 10, core i5@3.0GHz, 16Go RAM.

VII. What about using deterministic algorithm (SQP)

For optimization studies considering a large number of sizing parameters and constraints, the use of stochastic algorithms (such as NSGA-II) might raise computation time issues. Deterministic optimization algorithms are more adapted to consider specifications with a large number of parameters, but it raises the question of how to compute the derivatives?

VII.1 Jacobian computation

A great part of the presented modelling can be derivated without using finite differences:

- for the model of the machine, the derivatives of the outputs of the model with respect to every sizing parameters (machine geometry…) are computed using automatic code derivation with the ADOL-C tool, as it is implemented in C language and for simplicity;
- for the electrical drive circuit, the derivatives of the performance criteria according to each sizing parameters are computed using the method presented in (Gerbaud *et al.*, 2022) and (Diarra *et al.*, 2022);

- for the thermal model, it is the only part where derivatives are computed using finite differences at the present time, as it is numerically implemented in Java language without possible code derivation.

The computation of the overall model derivatives is obtained by derivative composition.

VII.2 COMPUTATION TIME COMPARISON

This enables to use deterministic algorithms, such as SQP, for the sizing by optimization of the system. However, the computation time of these derivatives will directly impact the size (number of parameters and constraints) and the complexity of the studied optimization problem. Table I presents a comparison of the model and Jacobian computation times, depending on which feature of the overall model is considered.

Table I: order of magnitude of model and Jacobian computation times, depending on the features considered.

	Electrical simulator	Electrical and thermal simulators
Model computation	10 – 100 ms	5 – 10 s
Jacobian computation	20 s	20 min
PC Windows 10, core i5@3.0GHz, 16Go RAM		

It can be seen that the addition of the thermal simulator has a significant impact on computation times, especially for the Jacobian. Thus, the use of finite differences at the present time to compute the derivatives reduces the interest in using gradient-based algorithms. A method for the computation of the exact derivatives should be implemented to solve that issue.

CONCLUSIONS

The paper focuses on a methodology for the sizing by optimization of an electrical drive, considering its dynamic heating. A multiphysics modelling of the different components of the drive is implemented. It is composed of three parts: a static electromagnetic model of the machine, a dynamic model of the electrical drive at steady state and a dynamic thermal model of the machine in transient state. The solving of the overall model is based on the co-simulation of two simulators (electrical and thermal) with master-slave relationship. The sizing by optimization approach is illustrated by an example using a genetic optimization algorithm. The computation of the derivatives of a great part of the modelling is implemented in order to enable the use of gradient-based algorithms, however, the computation of the thermal model gradients impacts strongly the overall Jacobian computation time.

In future works, a solution for the exact computation of the thermal model derivatives will be implemented to solve this issue. Moreover, an aid at the establishing of the state variables of the electrical drive circuit, and its derivatives, should be developed.

REFERENCES

Alger, P.L. (1970) “Induction Machines: Their behaviour and Uses”. Gordon and Breach, New York, NY.

Assaad, B., El kadri Benkara, K., Vivier, S., Friedrich, G., and Michon, A. (2017) "Thermal Design Optimization of Electric Machines Using a Global Sensitivity Analysis," *IEEE Transactions on Industry Applications*, vol. 53, no. 6, pp. 5365-5372, Nov.-Dec. 2017, doi: 10.1109/TIA.2017.2746015.

Baraston, A., Gerbaud, L., Reinbold, V., Boussey, T. and Wurtz, F. (2016). "Multiphysical approach including equivalent circuit models for the sizing by optimization", *COMPEL – The international journal for computation and mathematics in electrical and electronic engineering*, Vol. 35 No. 3, doi: 10.1108/COMPEL-11-2015-0418

Belot, A. (1982) “Calcul des fuites et inductances de fuites de l’induit”. *Techniques de l’Ingénieur*, September 10, 1982. doi: 10.51257/a-v1-d440

Boggs, P.T. and Tolle, J.W. (1995) “Sequential Quadratic Programming”. Acta Numer., vol. 4, p. 1-51, janv. 1995, doi: 10.1017/S0962492900002518.

Boglietti, A., Cavagnino, A. and Lazzari, M. (2011) "Computational Algorithms for Induction Motor Equivalent Circuit Parameter Determination—Part II: Skin Effect and Magnetizing Characteristics," in *IEEE Transactions on Industrial Electronics*, vol. 58, no. 9, pp. 3734-3740, Sept. 2011, doi: 10.1109/TIE.2010.2084975.

Boglietti, A., Cavagnino, A., Staton, D., Shanel, M., Mueller, M. and Mejuto, C. (2009) "Evolution and Modern Approaches for Thermal Analysis of Electrical Machines," in *IEEE Transactions on Industrial Electronics*, vol. 56, no. 3, pp. 871-882, March 2009, doi: 10.1109/TIE.2008.2011622

Bordry, F. and Foch, H. (1985), "Computer-aided analysis of power-electronic systems," *1985 IEEE Power Electronics Specialists Conference*, pp. 516-522, doi: 10.1109/PESC.1985.7070989.

Cheng, M., Isobe, T., Kato, S., Fukutani, K., Sumitani, H., Shimada, R. (2012). “Applying MERS for Induction Moter Driving”. *Journal of the Japan Institute of Power Electronics*. vol. 37, p. 139-145, doi: 10.5416/jipe.37.139.

Cochran, P. (1989) “Polyphase Induction Motors: Analysis, Design and Application”. CRC Press, New York, NY.

Cordovil, P. and Chabu, I. E. (2016) "Analytical calculation of slot leakage inductance in multiphase electrical machines," *2016 XXII International Conference on Electrical Machines (ICEM)*, pp. 1352-1358, doi: 10.1109/ICELMACH.2016.7732700.

Delinchant, B., Duret, D., Estrabaut, L., Gerbaud, L., Nguyen Huu, H., du Peloux, B., Rakotoarison, H.L., Verdiere, F., Wurtz, F. (2007) "An Optimizer using the Software Component Paradigm for the Optimization of Engineering Systems", *COMPEL, the international journal for computation and mathematics in electrical and electronic engineering*, Volume 26, Number 2, pp 368-379, doi: 10.1108/03321640710727728

Diarra, Z., Gerbaud, L., Chazal, H., Garbuio, L. (2022). “Sizing by SQP optimization of an electrical drive: Application to a switched capacitor connected to a permanent magnet synchronous generator”. *International Journal of Applied Electromagnetics and Mechanics*, 2022, 69 (3), pp.411-429, doi: 10.3233/JAE-210167.

Dormand, J.R., Prince, P.J. (1980). “A family of embedded Runge-Kutta formulae”. *Journal of Computational and Applied Mathematics*, Volume 6, Issue 1, 1980, Pages 19-26, doi: 10.1016/0771-050X(80)90013-3.

Fénot, M., Bertin, Y., Dorignac, E. and Lalizel, G. (2011). “A review of heat transfer between concentric rotating cylinders with or without axial flow”. *International Journal of Thermal Sciences*, Volume 50, Issue 7, Pages 1138-1155, doi: 10.1016/j.ijthermalsci.2011.02.013

Gerbaud, L., Diarra, Z.D., Chazal, H. and Garbuio, L. (2022) “Obtaining the most exact Jacobian for the time modelling of a power electronics structure to be used by gradient optimisation algorithms”, *COMPEL*, Vol. 41 No. 6, pp. 2096-2108, doi: 10.1108/COMPEL-10-2021-0398

Holman, J.P. (2010). “Heat Transfer”. McGraw-Hill Education, 10th edition, 758p, Jefferson City, MO.

Isobe, T., Wiik, J.A., Kitahara, T., Kato, S., Inoue, K., Arai, N., Usuki, K., Shimada, R. (2007) "Control of series compensated induction motor using magnetic energy recovery switch," *2007 European Conference on Power Electronics and Applications*, Aalborg, Denmark, 2007, pp. 1-10, doi: 10.1109/EPE.2007.4417774.

Kostenko, M.P. and Piotrovsky, L.M. (1969). “Electrical machines - Volume 2: alternating current machines", MIR, Moscow, Russia.

Liu, H., Ayat, S., Wrobel, R. and Zhang, C. (2019). “Comparative study of thermal properties of electrical windings impregnated with alternative varnish materials”. *The Journal of Engineering*, Vol. 2019, Issue 17, June 2019, doi: 10.1049/joe.2018.8198.

Liwschitz-Garik, M., Whipple, C. (1946). “Electric Machinery, Volume 1 and 2”. Van Nostrand, New York, NY.

Maddi, Z., Aouzellag. D. (2017) “Dynamic modelling of induction motor squirrel cage for different shapes of rotor deep bars with estimation of the skin effect” in *Progress In Electromagnetics Research* M. 59. 147-160, July 2017, doi: 10.2528/PIERM17060508

Mellor, P.H., Roberts, D. and Turner, D.R. (1991). « Lumped parameter thermal model for electrical machines of TEFC design », *IEE Proceedings B (Electric Power Applications)*, vol. 138, (5), p. 205-218, doi: 10.1049/ip-b.1991.0025.

Mezani, S., Takorabet, N. and Laporte, B. (2005) "A combined electromagnetic and thermal analysis of induction motors," in *IEEE Transactions on Magnetics*, vol. 41, no. 5, pp. 1572-1575, May 2005, doi: 10.1109/TMAG.2005.845044.

Mills, A.F. (1999). “Heat Transfer”, EngleWood Cliffs, Prentice-Hall, Upper Saddle River, NJ.

Press, W. H. Teukolsky, S. A. Vetterling, W. T. and Flannery, B. P. (1992) "Numerical Recipes in C, The Art of Scientific Computing", Second Edition, Cambridge university press

Staton, D., Boglietti, A. and Cavagnino, A. (2005) "Solving the more difficult aspects of electric motor thermal analysis in small and medium size industrial induction motors," in *IEEE Transactions on Energy Conversion*, vol. 20, no. 3, pp. 620-628, Sept. 2005, doi: 10.1109/TEC.2005.847979.

Touhami, S., Zeaiter, A., Fénot, M., Lefevre, Y., Llibre, J.F., Videcoq, E. (2020) “Electro-thermal Models and Design Approach for High Specific Power Electric Motor for Hybrid Aircraft Propulsion”, *Aerospace Europe Conference 2020*, Bordeaux, France.

Ulrich, K. and Eppinger, S. (2011). “Product Design and Development”, McGraw-Hill Education.

Zeaiter, A., Fénot, M., Saury, D. (2018). “Numerical Approach to Determining Windings’ Thermal Conductivity”. *2018 XIII International Conference on Electrical Machines (ICEM)*, Sep 2018, Alexandroupoli, Greece. pp.1291-1296, doi: 10.1109/ICELMACH.2018.8506692.

Zhu, Z.Q., Wu, L.J. and Xia, Z.P. (2010) "An Accurate Subdomain Model for Magnetic Field Computation in Slotted Surface-Mounted Permanent-Magnet Machines," in *IEEE Transactions on Magnetics*, vol. 46, no. 4, pp. 1100-1115, April 2010, doi: 10.1109/TMAG.2009.2038153.